

## ATLAS results on exotic hadronic resonances

---

**Evelina Bouhova-Thacker<sup>a,\*</sup> on behalf of the ATLAS Collaboration**

<sup>a</sup>*Lancaster University,*

*Lancaster, UK*

*E-mail:* [e.bouhova@cern.ch](mailto:e.bouhova@cern.ch)

Recent results from the proton-proton collision data taken by the ATLAS experiment at the Large Hadron Collider (LHC) on exotic resonances are presented. A search for  $J/\psi$   $p$  resonances in  $\Lambda_b \rightarrow J/\psi pK$  decays with large  $pK$  invariant masses is reported. Searches for exotic resonances in four-muon final states are also discussed.

*41st International Conference on High Energy Physics - ICHEP2022*

*6-13 July, 2022*

*Bologna, Italy*

---

\*Speaker

## 1. Introduction

Exotic hadrons composed of four ( $qq\bar{q}\bar{q}$ ) or five ( $qqqq\bar{q}$ ) quarks have been predicted by theory and provide a unique environment to study the strong interaction force and the confinement mechanism. A series of states consistent with containing four quarks have been discovered, while the existence of pentaquark states and their interpretation is not well established at present. Recent results from the ATLAS Collaboration [1] at the LHC on such exotic states are presented here.

## 2. Pentaquark searches in the $J/\psi p$ state

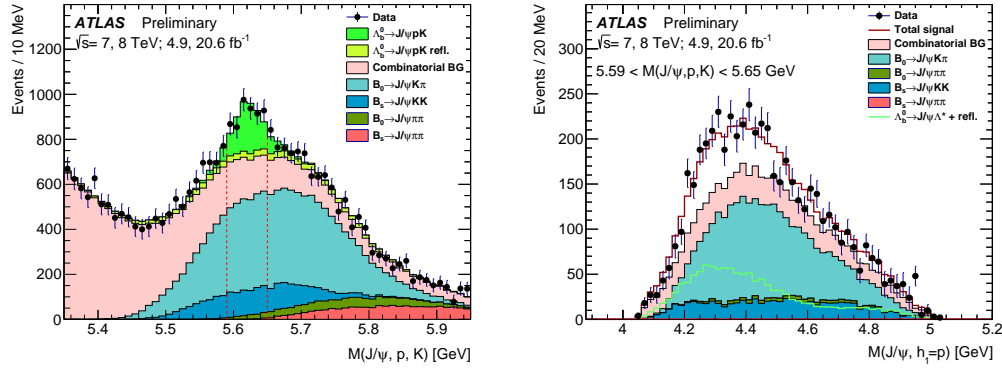
In 2015 the LHCb Collaboration [2] reported the observation of resonant structures in the  $J/\psi p$  invariant mass,  $M(J/\psi p)$ , in  $\Lambda_b \rightarrow J/\psi p K$  decays [3], which were interpreted as  $c\bar{c}uud$  pentaquark states. An amplitude analysis of the three-body final state yielded evidence for two resonances:  $P_c(4380)^+$  with a mass of  $4380 \pm 8 \pm 29$  MeV and a width of  $205 \pm 18 \pm 86$  MeV and a narrower one,  $P_c(4450)^+$ , with a mass of  $4449.8 \pm 1.7 \pm 2.5$  MeV and a width of  $39 \pm 5 \pm 19$  MeV. In a 2019 LHCb analysis [4], using an order of magnitude larger data sample and a binned  $\chi^2$  fit to the  $M(J/\psi p)$  distribution, the latter was resolved to two narrow states,  $P_c(4440)^+$  and  $P_c(4457)^+$ , with masses of  $4440.3 \pm 1.3^{+4.1}_{-4.7}$  MeV and  $4457.3 \pm 0.6^{+4.1}_{-1.7}$  MeV and widths of  $20.6 \pm 4.9^{+8.7}_{-10.1}$  MeV and  $6.4 \pm 2.0^{+5.7}_{-1.9}$  MeV, respectively. An additional narrow state  $P_c(4312)^+$  with a mass of  $4311.9 \pm 0.7^{+6.8}_{-0.6}$  MeV and a width of  $9.8 \pm 2.7^{+3.7}_{-4.5}$  MeV was also reported. The narrow resonances lie below the  $\Sigma_c \bar{D}^{(*)}$  thresholds and alternative explanations, other than pentaquark states, have not been ruled out.

ATLAS has published a study [5] of  $J/\psi p$  resonances in  $\Lambda_b \rightarrow J/\psi p K$  decays with large  $M(pK) > 2$  GeV invariant masses. The analysis is based on a combined sample of  $pp$  collision data at  $\sqrt{s} = 7$  TeV and 8 TeV corresponding to integrated luminosity of  $4.9 \text{ fb}^{-1}$  and  $20.6 \text{ fb}^{-1}$ , respectively. The signal decays,  $\Lambda_b \rightarrow J/\psi p K^- + h.c.$  are reconstructed and analysed alongside background processes as the ATLAS detector has no hadron particle identification. The well-established resonances contributing to  $\Lambda_b \rightarrow J/\psi p K$  decays are  $\Lambda^*(1800)$ ,  $\Lambda^*(1810)$ ,  $\Lambda^*(1890)$ ,  $\Lambda^*(2100)$  and  $\Lambda^*(2110)$ . Only the lowest orbital momenta between the  $\Lambda^*$  and  $P_c$  decay products are considered in the default model. The  $B^0 \rightarrow J/\psi K^+ \pi^-$  decays include contributions from light  $K^*$  states. Exotic  $B^0 \rightarrow Z_c X$  contributions have not been considered in the analysis, with the exception of  $B^0 \rightarrow Z_c(4200)^- K^+ \rightarrow J/\psi \pi^- K^+$ , where the effects of such a contribution are considered as systematic effects.  $B_s^0 \rightarrow J/\psi K^+ K^-$  decays include  $\phi$  and  $f_2$  states, while intermediate and non-resonant phase space decays are considered for  $B^0/B_s^0 \rightarrow J/\psi \pi^+ \pi^-$  decays.

Fits are performed to invariant mass distributions after subtracting same-sign background contributions, where both hadron tracks have the same charge. A 4-step iterative procedure is employed in multidimensional binned maximum likelihood fits, used to extract the parameters of the  $B^0$ ,  $B_s^0$  and combinatorial backgrounds, the total number of signal and background decays, the decay constants of the  $\Lambda_b$  decays, as well as the pentaquark masses, widths, amplitudes and the relative phase between the pentaquark amplitudes,  $\Delta\phi$ . The different dimensions in the fits correspond to the different hadron mass assignments.

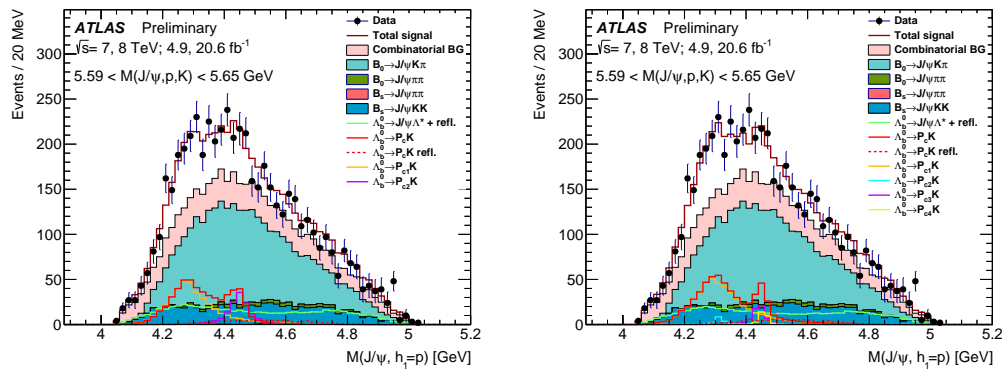
The  $M(J/\psi p K)$  distribution for all selected  $\Lambda_b$  candidates is shown in Figure 1 (left). The  $M(J/\psi p)$  distribution is analysed in the signal region,  $5.59 < M(J/\psi h_1 = p, h_2 = K) < 5.65$  GeV.

Figure 1 (right) shows the results of the  $\chi^2$  fit for the hypothesis without pentaquarks with the extended  $\Lambda_b \rightarrow J/\psi\Lambda^*$  decay model, which yields  $\chi^2/N_{\text{dof}} = 42.0/23$  and  $p\text{-value} = 9.1 \times 10^{-3}$ .



**Figure 1:** (left) Invariant mass for all selected  $\Lambda_b$  candidates [5], (right) results of the  $\chi^2$  fit [5] to the  $M(J/\psi p)$  distribution in the signal region without pentaquarks using the extended  $\Lambda_b \rightarrow J/\psi\Lambda^*$  decay model.

Figure 2 shows the results obtained from the fits including pentaquark states. The  $M(J/\psi p)$  distribution on the left shows the results for the hypothesis with two pentaquarks. The data description is good, with  $\chi^2/N_{\text{dof}} = 37.1/39$  and  $p\text{-value} = 55.7\%$ . The narrow pentaquarks reported by LHCb cannot be distinguished in the distribution due to the smaller number of signal candidates and the  $M(J/\psi p)$  resolution achieved. The pentaquark masses and widths obtained are consistent with the LHCb results within uncertainties. A fit with the two pentaquark masses and widths fixed to the LHCb values [3] yields  $\chi^2/N_{\text{dof}} = 49.0/43$  and  $p\text{-value} = 24.5\%$ . Figure 2 (right) shows the result of the fit with four pentaquarks with masses, widths and relative yields of the narrow pentaquarks fixed to the LHCb values [4]. The data description is also good, with  $\chi^2/N_{\text{dof}} = 37.1/42$  and  $p\text{-value} = 68.6\%$ . Although better fit results are achieved if pentaquark states are included, models without pentaquark states are still permitted.



**Figure 2:** Results of the  $\chi^2$  fits [5] to the  $M(J/\psi p)$  distribution in the signal region: (left) fit with two pentaquarks, (right) fit with four pentaquarks.

### 3. Tetraquarks in the four-muon final state

Evidence for a narrow resonance at 6.9 GeV in the di- $J/\psi \rightarrow 4\mu$  mass spectrum in LHCb data was reported in [6] and can be interpreted as a tetraquark with four charm quarks,  $T_{cc\bar{c}\bar{c}}$ . A broad structure next to the di- $J/\psi$  mass threshold, inconsistent with the hypothesis of non-resonant single-parton scattering (NRSPS) plus double-parton scattering (DPS) was also found. The mass and natural width of the narrow resonance obtained from a fit to the four-muon mass spectrum are  $m[X(6900)] = 6905 \pm 11 \pm 7$  MeV,  $\Gamma[X(6900)] = 80 \pm 19 \pm 33$  MeV, assuming no interference with the NRSPS continuum and  $m[X(6900)] = 6886 \pm 11 \pm 11$  MeV,  $\Gamma[X(6900)] = 168 \pm 33 \pm 69$  MeV with interference assumed.

ATLAS has performed a search for potential  $cc\bar{c}\bar{c}$  tetraquarks decaying into a pair of charmonium states in the four-muon final state [7] using  $pp$  collision data at  $\sqrt{s} = 13$  TeV corresponding to an integrated luminosity of  $139 \text{ fb}^{-1}$ .  $T_{cc\bar{c}\bar{c}} \rightarrow J/\psi J/\psi \rightarrow 4\mu$  and  $T_{cc\bar{c}\bar{c}} \rightarrow J/\psi \psi(2S) \rightarrow 4\mu$  decays are studied. Excess of events in data above the expected background is observed in both decay modes. The background consists of prompt di- $J/\psi$  (SPS and DPS) events, non-prompt di- $J/\psi$  from b-hadron decays, as well as events with a single charmonium plus fake muons or non-peaking background, containing no real charmonium candidates (the last two sources are denoted as "Others"). Figure 3 shows the  $4\mu$  mass distributions from data compared to the background predictions for the two channels.

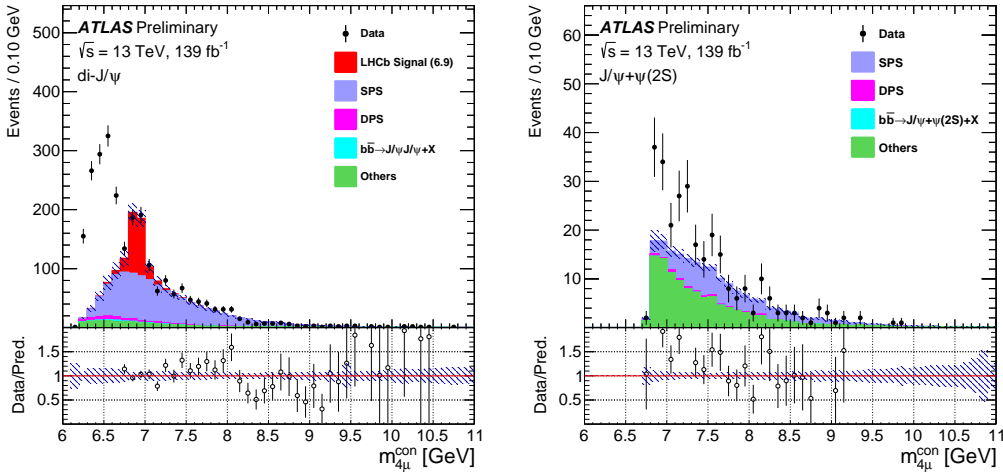


**Figure 3:** The  $4\mu$  mass spectra [7] in the di- $J/\psi$  (left) and  $J/\psi + \psi(2S)$  (right) channels.

Unbinned maximum likelihood fits are performed on the  $4\mu$  mass spectra with  $m_{4\mu} < 11$  GeV. A fit signal region ( $\Delta R < 0.25$ ) and a control region ( $\Delta R \geq 0.25$ ) are defined based on the angular separation of the two charmonia. The di- $J/\psi$  signal PDF consists of several interfering S-wave Breit-Wigner resonances, convolved with a mass resolution function  $R(\alpha)$ :

$$f_s(x) = \left| \sum_{i=0}^2 \frac{z_i}{x^2 - m_i^2 + im_i\Gamma_i} \right|^2 \sqrt{1 - \frac{4m_{J/\psi}^2}{x^2}} \otimes R(\alpha),$$

where  $m_i(\Gamma_i)$  are the masses (widths) of the resonances and  $z_i$  are complex numbers, representing the amplitudes. No interference between signal and the NRSPS background is assumed. Models with different number of resonances are compared in terms of  $\chi^2$  or toy Monte Carlo distributions.

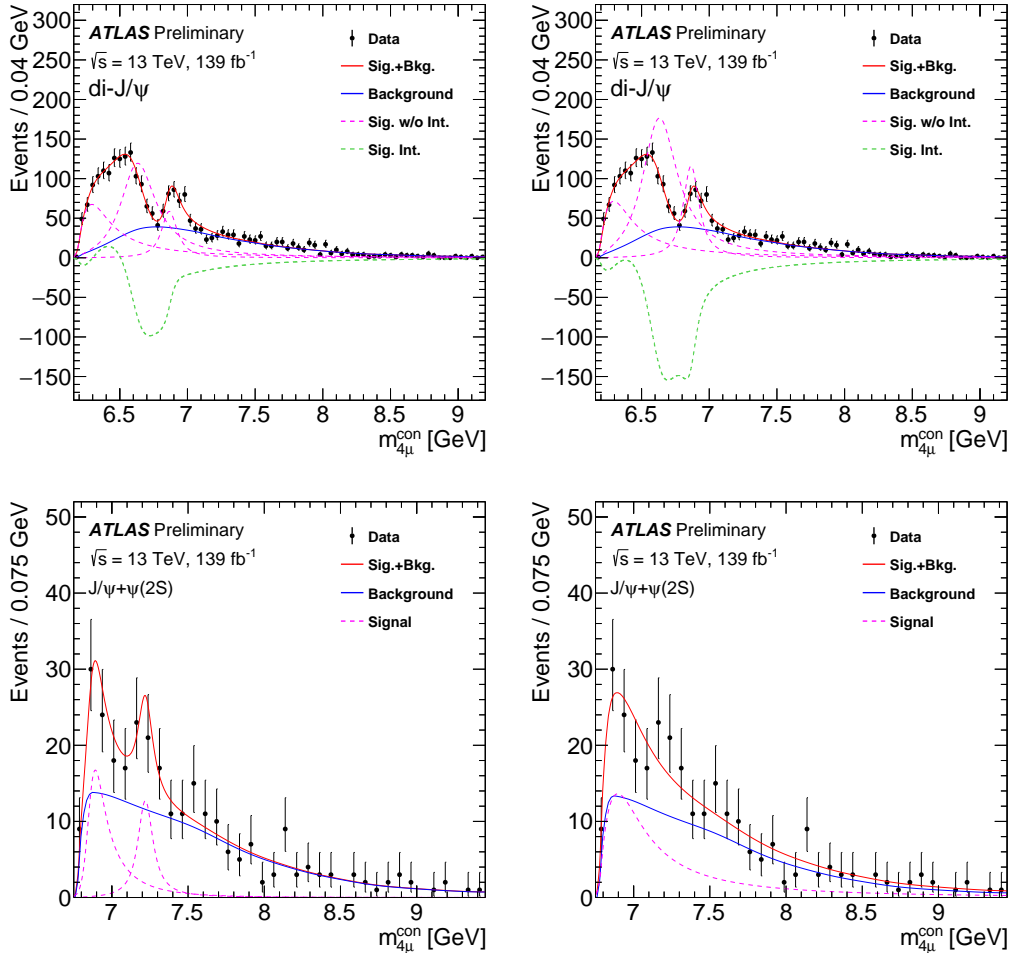


**Figure 4:** The fitted mass spectra [7] in the fit signal regions in the di- $J/\psi$  (top) and  $J/\psi + \psi(2S)$  (bottom) channels. The purple (green) dashed lines represent the components of individual resonances (interference among them). Two (out of four) degenerate solutions are shown for the di- $J/\psi$  channel. Model A (left) and Model B (right) fit results are shown for the  $J/\psi + \psi(2S)$  channel (see text for details).

Figure 4 (top) shows two of the four degenerate solutions to the three-resonance fit to data in the di- $J/\psi$  channel. The other two solutions are very close to the ones shown. The obtained values for the resonance masses and widths are:  $m_0 = 6.22 \pm 0.05^{+0.04}_{-0.05}$  GeV,  $\Gamma_0 = 0.31 \pm 0.12^{+0.07}_{-0.08}$  GeV,  $m_1 = 6.62 \pm 0.03^{+0.02}_{-0.01}$  GeV,  $\Gamma_1 = 0.31 \pm 0.09^{+0.06}_{-0.11}$  GeV and  $m_2 = 6.87 \pm 0.03^{+0.06}_{-0.01}$  GeV,  $\Gamma_2 = 0.12 \pm 0.04^{+0.03}_{-0.01}$  GeV. The mass of the third resonance is consistent with the LHCb result for  $X(6900)$  and its significance is  $10\sigma$ . The fit quality of the two-resonance fit is about 70% worse than the three-resonance fit. A fit with the mass and width of the third resonance fixed to the LHCb Model I values gives similar results as the three-resonance fit, while a fit with LHCb Model II

(including interference with NRSPS and no  $\Delta R$  cut) is disfavoured based on the fit quality. None of the attempted fits include feed-down from  $J/\psi + \psi(2S)$  or higher di-charmonium resonances.

In the  $J/\psi + \psi(2S)$  channel, two fit models are considered: the first one, Model A assumes the same interfering resonances as in the di- $J/\psi$  fit plus an additional standalone resonance. The parameters of the first three resonances are fixed to the di- $J/\psi$  fitted values. As these terms have masses  $m_i$  below  $m_{J/\psi} + m_{\psi(2S)}$ , their contribution appears as a broad structure just above the  $J/\psi + \psi(2S)$  mass threshold. The second model, Model B assumes a single resonance. In both cases, no interference between signal and the NRSPS background is assumed.

Figure 4 (bottom) shows the results from the fits to the  $J/\psi + \psi(2S)$  four-muon mass distribution. A  $4.6\sigma$  ( $4.3\sigma$ ) excess of events is observed in the case of Model A (B). The values for the mass and width of the resonance in Model B are  $m = 6.78 \pm 0.36^{+0.35}_{-0.54}$  GeV and  $\Gamma = 0.39 \pm 0.11^{+0.11}_{-0.07}$  GeV. The significance of the additional resonance in Model A, with mass  $m_3 = 7.22 \pm 0.03^{+0.02}_{-0.03}$  GeV and width  $\Gamma_3 = 0.10^{+0.13+0.06}_{-0.07-0.05}$  GeV, is  $3.2\sigma$ . A hint for such a structure at 7.2 GeV was also noted by LHCb [6]. More data are needed to confirm its existence.

The analysis of ATLAS data corroborates the existence of a resonance around 6.9 GeV decaying into a pair of charmonium states in the four-muon final state. The best description in the di- $J/\psi$  channel is given by a three-resonance model with interference. In both channels the details of the lower-mass structure cannot be discerned directly from the data, other interpretations, such as multiple non-interfering resonances, reflection effects and threshold enhancements, cannot be excluded. More data are required to better characterise the excesses observed in both channels.

## References

- [1] ATLAS Collaboration, *The ATLAS Experiment at the CERN Large Hadron Collider*, *JINST* **3** (2008) S08003.
- [2] LHCb Collaboration, *The LHCb Detector at the LHC*, *JINST* **3** (2008) S08005.
- [3] LHCb Collaboration, *Observation of  $J/\psi p$  resonances consistent with pentaquark states in  $\Lambda_b^0 \rightarrow J/\psi p$  decays*, *Phys. Rev. Lett.* **115** (2015) 072001.
- [4] LHCb Collaboration, *Observation of a narrow pentaquark state,  $P_c(4312)^+$ , and of two-peak structure of the  $P_c(4450)^+$* , *Phys. Rev. Lett.* **122** (2019) 222001.
- [5] ATLAS Collaboration, *Study of  $J/\psi p$  resonances in the  $\Lambda_b^0 \rightarrow J/\psi p$  decays in  $pp$  collisions at  $\sqrt{s} = 7$  and 8 TeV with the ATLAS detector*, Report No. ATLAS-CONF-2019-048 (2019), <https://cds.cern.ch/record/2693957>.
- [6] LHCb Collaboration, *Observation of structure in the  $J/\psi$ -pair mass spectrum*, *Science Bulletin* **65** (2020) 1983.
- [7] ATLAS Collaboration, *Observation of an excess of di-charmonium events in the four-muon final state with the ATLAS detector*, Report No. ATLAS-CONF-2022-040 (2022), <https://cds.cern.ch/record/2815676>.